

# Magnetic Anisotropy and Morphology of Fe Epitaxial Layers Grown on MgO/InAs Heterostructures

Kyung-Ho Kim<sup>1,2</sup>, Hyung-jun Kim<sup>1,\*</sup>, Jae-Pyung Ahn<sup>3</sup>, Jun-Hyun Han<sup>4</sup>,  
Jun Woo Choi<sup>1</sup>, and Joonyeon Chang<sup>1</sup>

<sup>1</sup>Spin Device Research Center, Korea Institute of Science and Technology, Seoul 136-791, Korea.

<sup>2</sup>Department of Advanced Materials Science and Engineering, Korea University, Seoul 136-713, Korea.

<sup>3</sup>Advanced Analysis Center, Korea Institute of Science and Technology, Seoul 136-791, Korea.

<sup>4</sup>Department of Nano Materials Engineering, Chungnam National University, Daejeon 305-764, Korea.

In-plane magnetic anisotropy and the corresponding morphology of Fe epitaxial layers have been investigated with respect to underlying MgO growth temperature when epitaxial Fe/MgO layers are grown on InAs (001) substrates. Coexistence of three-dimensional Fe islands with strong in-plane textures along (110) and (100) is observed on 4 nm thick MgO layers grown on 200 °C, leading to the absence of magnetic anisotropy. Meanwhile, the partially relaxed MgO layers grown above 300 °C give rise to two-dimensional Fe layers with cubic magnetic anisotropy. The higher MgO growth temperature accelerates the two-dimensional layer formation of the subsequent Fe as well as the advent of cubic anisotropy by reducing underlying strain within the MgO layer.

**Keywords:** Morphology, Strain, In-Plane Magnetic Anisotropy, Epitaxial Relationship.

## 1. INTRODUCTION

Efficient spin injection from a ferromagnetic (FM) material into a semiconductor (SC) is significantly essential for the implementation of spin-based electronic devices. Utilizing a tunnel barrier increases spin injection polarization by reducing the conductivity mismatch between FM and SC.<sup>1</sup> In particular, the insertion of an MgO tunnel barrier at the FM/SC interface has been of great interest because the crystalline MgO gives rise to high spin filtering effect through coherent tunneling process.<sup>1–3</sup>

Recently the realization of a gate modulated spin-field effect transistor (spin-FET) has been reported using an InAs quantum well (QW) structure.<sup>4</sup> The InAs is a promising semiconductor for the spin-FET because it is a narrow gap semiconductor with high electron mobility and strong spin-orbit interaction (SOI), which are prerequisite to control spin precession by gate electric field.<sup>5</sup> The heterostructure of Fe/MgO/InAs has attracted great attention as a favored candidate for spin-based electronic device applications.<sup>1,6</sup> However, the study on the correlation between Fe morphology and the corresponding magnetic anisotropy is lacking when the Fe/MgO layers are grown on InAs (001) substrates. It is well established that the magnetic anisotropy of an epitaxial Fe layer grown directly on a GaAs (001) substrate is influenced by many

factors such as crystal structure, thickness, morphology, and interfacial strain.<sup>7–9</sup> Nevertheless, the origin of the unexpected uniaxial anisotropy of a thin Fe layer has not been completely understood.

Many recent studies reported the different shapes of Fe islands when grown on MgO (001) substrates.<sup>10–12</sup> The substrate temperature differentiates the Fe island shape which is related with the strain relief and adatom surface diffusion. However, there has been insufficient study on the corresponding magnetic anisotropy of the Fe islands.

In this study, we have investigated the magnetic anisotropy of Fe with the corresponding morphology change manipulated by the growth temperature of the underlying MgO layer. The experimental results obtained from Fe/MgO/InAs heterostructure allow us to further understand the key correlation between the morphology and magnetic property for the enhanced spin-FET device performance.

## 2. EXPERIMENTAL METHODS

All of the Fe/MgO/InAs heterostructures were fabricated using a cluster molecular beam epitaxy (MBE) system composed of two separated MBEs and a magnetron sputter unit. The epitaxial layers of an InAs buffer, MgO, and Fe were subsequently grown without vacuum break, ensuring the exclusion of native oxide formation at the interfaces.

\* Author to whom correspondence should be addressed.

After semi-insulating InAs (001) substrates were introduced into a MBE system, surface oxide layers were thermally removed by heating up to 480 °C. A 300 nm thick InAs buffer layer was grown to obtain streaky ( $2 \times 4$ ) As-terminated surface. The growth temperature of 4 nm thick MgO layer was changed as a key experimental parameter in the range from-room temperature (RT) to 400 °C. The growth temperature of the subsequent 7 nm thick Fe was kept constant at 200 °C. Although the incident Fe beam was at the angle of about 37° to the substrate surface in our growth geometry, there is no effect of the oblique incidence due to the substrate rotation at 10 rpm. Al capping layers were finally grown on all the samples at RT to prevent oxidation of Fe at atmosphere.

The microstructural evolutions of MgO and Fe were characterized by a high resolution transmission electron microscope (HRTEM, Titan) operated at 300 kV and a X-ray diffractometer (Phillips X'Pert) with Cu K $\alpha$  radiation ( $\lambda = 1.7902 \text{ \AA}$ ). In particular, the Fe morphology was carefully observed in plane-view and cross-section HRTEM with selected area diffraction (SAD) patterns. The in-plane magnetic anisotropies of Fe were *ex situ* measured using by an alternating-gradient magnetometer (AGM) with sensitivity up to  $10^{-9}$  emu.

### 3. RESULTS AND DISCUSSION

The Fe morphology and crystalline structure are examined in the Fe/MgO/InAs heterostructures grown at different MgO growth temperatures of RT, 100, 200, 300, and 400 °C, respectively. As the MgO growth temperature increases, the slight ring-like component in reflection high-energy electron diffraction (RHEED) patterns of Fe disappear and the spots become brighter above 100 °C. Figure 1 shows the HRTEM images and SAD patterns observed from the Fe/MgO/InAs heterostructures of two representative MgO growth temperatures of 200 °C and 300 °C, respectively. The 2D MgO layers grown at the two different temperatures retain single crystalline structures as shown in the insets of Figures 1(a and c). It is worth noting that three-dimensional (3D) Fe islands on the MgO layers grown below 200 °C are completely suppressed and two-dimensional (2D) Fe epitaxial layer forms on the MgO layers grown above 300 °C. The cross-sectional and plane-view HRTEM images of Figures 1(a–d) evidently illustrate the Fe morphology evolution. As the MgO growth temperature increases from RT to 200 °C, the density and aspect ratio of the Fe islands decrease as like quantum dots of less lattice mismatching to substrates.<sup>13</sup> As described in our previous work, the formation of Fe islands results from the underlying strain caused by the large lattice mismatch of about 7.7% between MgO and InAs substrate.<sup>14</sup> This underlying strain is partially relaxed when the MgO layers are grown at the high growth temperatures. As a result, the epitaxial Fe layer forms due to the relatively reduced

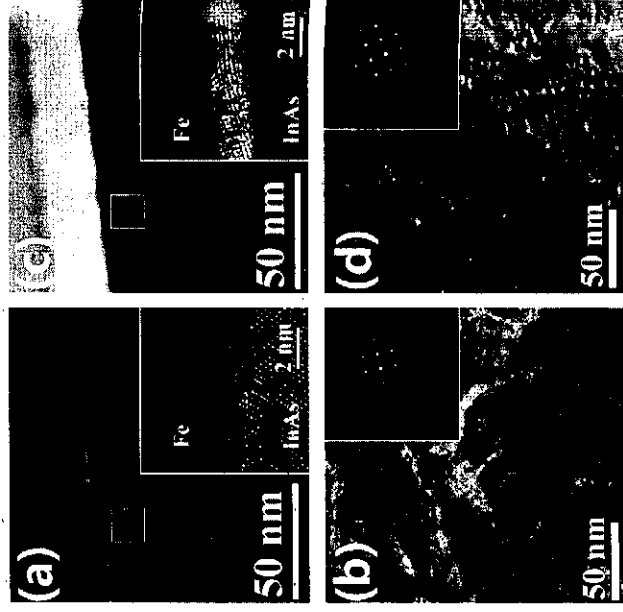


Fig. 1. HRTEM images and the corresponding SAD patterns of Fe/MgO/InAs heterostructures of the MgO layer grown at 200 °C (left column) and 300 °C (right column). (a) and (c); cross-sectional images and (b) and (d); plane-view images. The insets in (a) and (c) are the corresponding HRTEM images of higher magnification showing the crystal structures of MgO and Fe. The insets in (b) and (d) are SAD patterns obtained from the plane-view images.

lattice mismatch. As shown in Figures 1(a and b), the HRTEM images of the Fe/MgO(200 °C)/InAs heterostructure show the Fe islands of serpentine shape with about 5 nm spacing. The elemental mapping of the plane-view HRTEM image ensures that the Fe islands are completely separated by the underlying MgO surface (not shown) which probably indicating Volmer-Weber growth mode. On the other hand, the 7 nm thick Fe on the MgO grown at 300 °C grows in 2D epitaxial layer with Morie fringes. The SAD patterns of the insets in Figures 1(b and d) display the bright spots of the InAs substrate and the crystalline Fe. The 4 nm thick MgO used in this study is too thin to obtain the diffraction patterns.

In contrast to the diffraction spots from the Fe layer shown in the inset of Figure 1(d), the Fe islands show four diffuse spots in the inset of Figure 1(b), indicating that two perpendicular directions  $[110]$  and  $[\bar{1}\bar{1}0]$  is in-plane rotated by about 7° each other. This experimental observation signifies that the Fe islands are misoriented with the strong textures while the Fe layer possesses the well known epitaxial relationship of Fe $[010]$ /MgO $[\bar{1}10]$ /InAs $[\bar{1}\bar{1}0]$ .<sup>14</sup>

The origin of the diffuse spots from the Fe islands is uncertain. Presumably it results from that individual Fe islands are polycrystalline or single crystalline Fe islands are in-plane misoriented. XRD analysis is performed in the larger surface area of the Fe/MgO/InAs heterostructure of the MgO growth temperature of 200 °C to verify the origin. Figure 2 shows the  $\theta$ - $2\theta$  scan and  $\phi$ -scans obtained

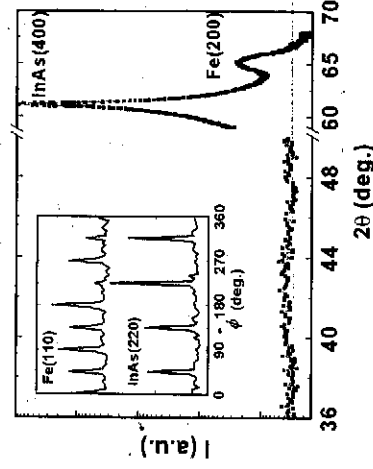


Fig. 2. XRD  $\theta$ - $2\theta$  scan of Fe/MgO/InAs heterostructure of the MgO layer grown at 200 °C. The inset is  $\phi$ -scans for Fe(110) and InAs(220).

from the heterostructure of the MgO growth temperature of 200 °C. The peaks corresponding Fe(200) and InAs(400) reflections are clearly observed but MgO peak is not seen due to the relatively thin thickness. The presence of only Fe(200) orientation clearly supports the epitaxy of the Fe islands in the surface normal direction. The  $\phi$ -scans in the inset of Figure 2 show the interesting in-plane epitaxial relationship of the Fe islands. Fe(110) reflections display eight characteristic peaks at 45° interval. This experimental observation verifies that two different in-plane textures of (110) and (100) coexist in the Fe islands. In other words, the Fe islands on the MgO grown at 200 °C are distributed with 0° and 45° in-plane rotation with respect to the underlying MgO. Our XRD results point out that the individual Fe islands are single crystalline with the different in-plane misorientation on the MgO layer grown on 200 °C.

Next, in order to examine the in-plane magnetic anisotropy with respect to the Fe morphologies of the Fe islands and the Fe layer, the Fe/MgO/InAs heterostructures grown at the different MgO growth temperatures were measured by AGM. Magnetic hysteresis loops were taken with the applied magnetic field in the four major in-plane directions [100], [110], [110] and [110]. Although the nominal 7 nm thick Fe in the two heterostructures shows ferromagnetism, there is a considerable contrast in magnetic hysteresis loop between the Fe islands and the Fe layer.

Figure 3 illustrates the M-H hysteresis loops of two representative heterostructures with the typical MgO growth temperatures of 200 °C and 300 °C, respectively. It is surprising that there is no magnetic anisotropy in the Fe islands while the Fe layer represents the cubic anisotropy with the easy axis along (100) direction. Note that the Fe (100) easy axis is parallel to (110) axes of both underlying MgO and InAs substrate. If the Fe islands are polycrystalline, it is no wonder that the Fe islands on the MgO grown at 200 °C display no magnetic anisotropy. However, the experimental XRD results evidently reveal that the in-plane misorientations of single crystalline Fe islands are the direct reason of no magnetic anisotropy. Another possible reason of no magnetic anisotropy is that the large

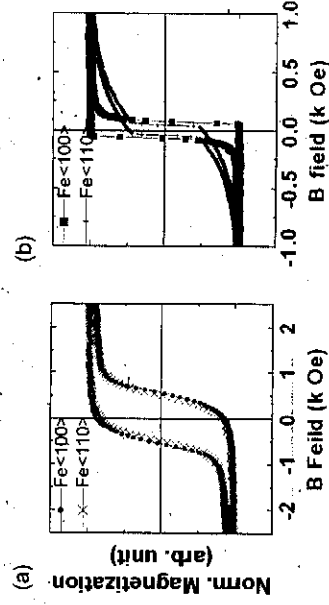


Fig. 3. AGM hysteresis loops of Fe/MgO/InAs heterostructures of (a) 3D Fe islands on the MgO layer grown at 200 °C and (b) 2D Fe layer on the MgO layer grown at 300 °C.

coercive field and non-square M-H hysteresis loops in Figure 3(a) imply that the individual Fe islands shown in Figure 1(b) could possess magnetic single domains.<sup>15</sup> Thus, the magnetic anisotropy of the individual Fe islands would cancel out and the entire Fe islands show no magnetic anisotropy.

#### 4. CONCLUSIONS

In conclusion, we experimentally demonstrate the morphology-magnetic anisotropy correlation of Fe in Fe/MgO/InAs heterostructures with respect to the MgO growth temperature. It is found that the nominal 7 nm thick Fe on the MgO layer grown at the growth temperatures below 200 °C shows 3D island formation with no magnetic anisotropy due to the in-plane misorientation of the single crystalline Fe islands. In contrast, the MgO layer grown at the higher growth temperatures give rise to the 2D Fe layer of cubic anisotropy with the easy axis along (100) direction of Fe lattice. The Fe morphology and the corresponding magnetic anisotropy are remarkably influenced by the underlying strain within MgO layer originated from the lattice mismatch between MgO and InAs substrate. The MgO growth temperature used in this study is one of the most important key factors determining the underlying strain. The partially strain relaxed MgO grown at the high growth temperatures accelerate not only the 2D layer formation of subsequent Fe but also the advent of the cubic anisotropy.

**Acknowledgment:** This work was supported by the Korea Institute of Science and Technology (KIST) Institutional Program, the Degree and Research Center (DRC) Program funded by the Korea Research Council of Fundamental Science and Technology (KRCF), IT R&D program of MKE/KEIT (2009-F-004-01, Technology Development of 30 nm level High Density Perpendicular STT-MRAM), and the National Research Foundation of Korea (NRF) grant funded by the Korea government (MEST) (No. 2011-0016471).

## References and Notes

1. X. Jiang, R. Wang, R.-M. Shelby, R. M. Macfarlane, S. R. Bank, J. S. Harris, and S. S. P. Parkin, *Phys. Rev. Lett.* **94**, 056601 (2005).
2. H. J. Zhu, M. Wässemeier, H.-P. Schönherr, and K. H. Ploog, *Phys. Rev. Lett.* **87**, 016601 (2001).
3. R. Wang, X. Jiang, R. M. Shelby, R. M. Macfarlane, S. S. P. Parkin, S. R. Bank, and J. S. Harris, *Appl. Phys. Lett.* **86**, 052901 (2005).
4. H. C. Koo, J. H. Kwon, J. H. Eom, J. Y. Chang, S. H. Han, and M. Johnson, *Science* **325**, 1515 (2009).
5. T. Akazaki, J. Nitta, H. Takayangi, T. Enoki, and K. Arai, *Appl. Phys. Lett.* **65**, 1263 (1994).
6. G. X. Miao, J. Y. Chang, M. J. van Veenhuizen, K. Thiel, M. Seibt, G. Eilers, M. Münzenberg, and J. S. Moodera, *Appl. Phys. Lett.* **93**, 142511 (2008).
7. Y. B. Xu, E. T. M. Kernohan, D. J. Freeland, A. Ercole, M. Tselepi, and J. A. C. Bland, *Phys. Rev. B* **58**, 890 (1998).
8. E. M. Kneedler, B. T. Jonker, P. M. Thibado, R. J. Wagner, B. V. Shanabrook, and L. J. Whitman, *Phys. Rev. B* **56**, 8163 (1997).
9. J. Lindner, C. Hassel, A. V. Trunova, F. M. Römer, S. Stienen, and I. Barsukov, *J. Nanosci. Nanotechnol.* **10**, 6161 (2010).
10. J. F. Lawler, R. Schad, S. Jordan, H. Van Kempen, *J. Magn. Magn. Mater.* **165**, 224 (1997).
11. M. Mizuguchi, Y. Suzuki, T. Nagahama, and S. Yuasa, *J. Nanosci. Nanotechnol.* **7**, 255 (2007).
12. G. Wedler, C. M. Schneider, A. Trampert, and R. Koch, *Phys. Rev. Lett.* **93**, 236101 (2004).
13. H. J. Kim and Y. H. Xie, *Appl. Phys. Lett.* **79**, 263 (2001).
14. K. H. Kim, H. J. Kim, G. H. Kim, J. Y. Chang, and S. H. Han, *Appl. Phys. Lett.* **95**, 164103 (2009).
15. X. X. Zhang, G. H. Wen, S. Huang, L. Dai, R. Gao, and Z. L. Wang, *J. Magn. Magn. Mater.* **231**, L9 (2001).

Received: 3 September 2010. Accepted: 2 December 2010.